Flexible Resource Optimization for GEO Multibeam Satellite Communication System

Tedros Salih Abdu^{ORCID}, *Graduate Student Member, IEEE*, Steven Kisseleff^{ORCID}, *Member, IEEE*, Eva Lagunas^{ORCID}, *Senior Member, IEEE*, and Symeon Chatzinotas^{ORCID}, *Senior Member, IEEE*

Abstract— **Conventional GEO satellite communication systems rely on a multibeam foot-print with a uniform resource allocation to provide connectivity to users. However, applying uniform resource allocation is inefficient in presence of non-uniform demand distribution. To overcome this limitation, the next generation of broadband GEO satellite systems will enable flexibility in terms of power and bandwidth assignment, enabling on-demand resource allocation. In this paper, we propose a novel satellite resource assignment design whose goal is to satisfy the beam traffic demand by making use of the minimum transmit power and utilized bandwidth. The motivation behind the proposed design is to maximize the satellite spectrum utilization by pushing the spectrum reuse to affordable limits in terms of tolerable interference. The proposed problem formulation results in a non-convex optimization structure, for which we propose an efficient tractable solution. We validate the proposed method with extensive numerical results, which demonstrate the efficiency of the proposed approach with respect to benchmark schemes.**

Index Terms— **Flexible GEO satellite, carrier allocation, power allocation, demand matching.**

I. INTRODUCTION

THE application of satellite communications (SatCom) has recently evolved from providing a simple Direct-To-Home television (DTHTV) to enabling a span of broadband internet services [2]. Furthermore, SatComs have an important role in providing ubiquitous connectivity to the maritime and aeronautical markets, as well as to remote areas with non-existing or expensive connectivity to the terrestrial networks [3]. Current GEO broadband SatCom systems rely on a multibeam foot-print with a low fractional frequency reuse pattern that helps to improve the spectrum utilization while keeping the inter-beam interference under acceptable

levels. Typically, the bandwidth and power allocation is done uniformly across beams, leading to equal offered capacity per beam [4], [5]. Recent studies have shown that this uniform allocation is extremely inefficient in practical scenarios with heterogeneous traffic demands, since the demand observed in some beams may exceed the available beam capacity, while in others the situation is the opposite [6], [7]. Furthermore, the current GEO broadband SatCom systems are facing challenges arising from the following aspects:

- *Spectrum Congestion:* With the emerging new space actors, namely the Non-GSO constellations with thousands of small satellites being launched, there is an increasing demand on the already limited spectrum [8]. Therefore, satellite operators have to assume that the spectrum that is made available for their operations is limited and it is important to make the most out of it in order to maximize the economic yield while satisfying the customers contracts in terms of offered capacity.

- *Power Consumption:* Power consumption has been traditionally a major limitation in satellite systems, as it has an impact on the mass and lifetime of the satellite [9]. With the forthcoming on-board beamforming technology, which is significantly power-hungry, on-board power optimization is becoming a major concern. Therefore, innovative techniques must be implemented in order to reduce the power consumption and one feasible way is to reduce the transmit power [10].

In response to the above challenges as well as to the heterogeneous traffic demand patterns, the next generation of SatCom systems considers the deployment of a full digital payload combined with software-defined adaptive resource management. This revolution in the space segment opens a door to advanced resource management techniques capable of maximizing the satellite resource utilization while dynamically matching the distribution of the satellite capacity on ground to the geographic distribution of the traffic demand [11]–[13]. Currently, more sophisticated satellite designs with adaptive resource assignment capabilities are in the making or in testing phase. As an example, the upcoming SES-17 [14] (built by THALES) and recently launched EUTELSAT QUANTUM [15] represent the major projects taking place in Europe in this regard. While technology is mature enough, the actual algorithmic part to optimally exploit such technology is in lower stages of maturity. For instance, SES has recently partnered with Kythera Space Solutions to develop a

software system to dynamically synchronise space and ground resource [16]. In addition, minimizing the satellite power consumption is a fundamental aspect, particularly for the upcoming digitally-controlled payloads with on-board active antenna systems [9], [17], [18].

Flexible satellite resource allocation strategies for the demand matching problem have recently attracted attention from the research community. A bandwidth allocation based on a greedy algorithms with Spatial Division Multiple Access (SDMA) technique have been proposed in [19], where the bandwidth is assigned to users based on the cumulative interference levels. Similarly, the bandwidth allocation based on beam traffic demand has been addressed in [20], where a heuristic approach is proposed to adjust the bandwidth of each beam while minimizing the difference between the traffic demand and the offered capacity. In addition, [20] proposes an active beam selection algorithm to further increase the overall system capacity. The limitation of [20] is that inter-beam interference has been neglected.

The power optimization based on demand and channel quality has been considered in [21], where the goal is the overall system performance as well as achieving reasonable fairness among users. Similarly, power allocation with the objective of maximizing the energy efficiency (EE) is presented in [22], where the modeling includes the effect of imperfect channel state information. Again, the main drawback of [21], [22] is that the inter-beam interference has not been considered. Additionally, power allocation methods have been studied in [18], [23]–[25] considering the conventional 4-color frequency reuse pattern, where inter-beam interference is minimized at the cost of spectral efficiency.

A joint power and frequency allocation has been introduced in [26] focusing on the maximization of the minimum ratio between the requested and the offered SINR. The authors extended [26] in [27] by proposing a maximization of the total capacity allocated with respect to the requested traffic. The flexibility of [26], [27] is however limited by the assumption on orthogonal carrier assignment within a beam cluster and a binary power allocation, i.e. $\{0, P_{\max}\}$.

Targeting the minimization of the unmet system capacity, computationally expensive joint optimization techniques have been proposed in [28], [29]. In [29], the resulting non-convex optimization problem is solved using a modified version of the simulated annealing algorithm. On the other hand, [28] extends [18] to the frequency assignment by employing an hybrid genetic algorithm and simulated annealing method.

The benefits of joint power and time flexibility are explored in [27], [30], [31] by considering Beam-Hopping (BH). In BH, all satellite resources are employed to provide service to a certain subset of beams, which is active for some portion of time. In this paper, frequency flexibility is preferred to time flexibility to avoid synchronization aspects related to the terminal switching on/off and potential latency issues associated with the bursty transmissions. Furthermore, the Digital Transparent Processor (DTP) payloads are more mature than BH payloads.

Some of the existing works also consider precoding techniques to reduce the inter-beam interference when the system

TABLE I
COMPARISON OF SCHEMES

Schemes	Objective Function			Flexibility	
	Demand Matching	Total Power Minimization	Utilized BW Minimization	Carrier	Power
[20]	✓			✓	
[26], [27]	✓			✓	
[30]	✓			✓	
[23]					✓
[25]	✓				✓
[28]	✓			✓	✓
[29]	✓			✓	✓
[22]		✓			✓
[9]	✓	✓			✓
[18]	✓	✓			✓
This Work	✓	✓	✓	✓	✓

uses full frequency reuse. The utilization of full frequency reuse with precoding techniques substantially increase the spectral efficiency of the system [32]–[36]. However, the goal of this manuscript is to shed some light onto the limits of a flexible GEO satellite system without precoding capabilities which are require the upgrade of Gateway (GW) and User Terminals (UTs).

Table I shows a comparison of the resource allocation schemes encountered in the literature in terms of the optimization objective (demand matching or/and total power minimization) and the satellite resource flexibility (power or/and frequency).

Unlike previous works mentioned in the Table I, herein we propose a flexible resource optimization method to satisfy the heterogeneous traffic demand while maximizing the satellite resource utilization. In particular, the minimization of the number of frequency carriers and transmit power required to match the predetermined beam demand is the focus of this paper. Note that the main contribution of this work relies on a novel system optimization perspective that allows the system to utilize more efficiently the power and the bandwidth of the satellite with the objective of using as few carriers and less power as possible while satisfying the demand. In fact, the formulation of the proposed optimization problem targets a different goal than those of the existing papers, which is aligned with the relevant satellite operator concerns. The detailed contributions of this paper are summarized as follows:

- We formulate an optimization problem for the carrier and power assignment enforcing the design to use as few carriers and less power as possible. Note that the resulting assignment may consider frequency re-use across beams. However, the proposed approach allows certain interference as far as the supplied capacity is above the requested demand.

- The formulated optimization problem renders a non-convex structure, for which we proposed a two-step tractable approach. First, we estimate the number of frequency carriers and the power-per-carrier required for each beam to satisfy its demand. For this, we propose two techniques: (i) The Contiguous Carrier Assignment (CCA) [1] and (ii) the Interference Aware Carrier Assignment (IACA), which considers a non-adjacent carrier assignment that minimizes the maximum inter-beam
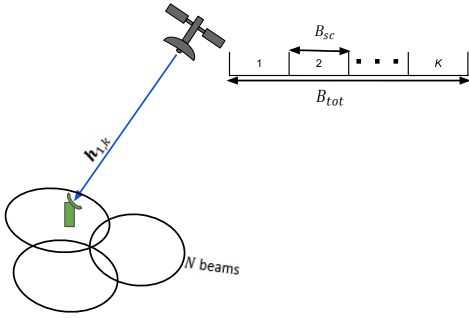
Fig. 1. Specific spectrum block shared among users per group.

interference component of the systems. Finally, we optimize the power allocation based on the previously assigned carriers. Difference-of-Convex-Functions (DC) and Successive Convex Approximation (SCA) are used to tackle the optimization problems encountered in this part.

- A detailed complexity analysis is provided for each of the steps involved in the proposed solution.
- Finally, the performance of the proposed algorithm is demonstrated via extensive numerical results. It is shown that the proposed scheme significantly outperforms the benchmark schemes in terms of demand matching, average used power and bandwidth utilization.

The rest of the paper is organized as follows. In Section II, the system model for the GEO satellites with flexible resource allocation capabilities is described. The problem formulation and the proposed solution for carrier and power allocation is presented in Section III. In Section IV, the numerical results are discussed. Subsequently, Section V concludes the paper.

Notation: Boldface of upper case and lower case letters refers to matrices and vectors, respectively. The symbol $\lceil \cdot \rceil$ denotes the ceiling function. The transpose of a vector and conjugate transpose of a vector represented by $[.]^T$ and $[.]^H$, respectively. Lastly, $\mathbb{E}[.]$ and diag(.) represents the expected value and a diagonal matrix, respectively.

II. SYSTEM MODEL

We consider a downlink multibeam GEO satellite system with N beams and K carriers ($\mathcal{K} = \{1, 2, \ldots, K\}$), as illustrated in Fig. 1. The total available system bandwidth is denoted as B_{tot} while the carrier bandwidth is denoted as B_{sc}, such that $B_{tot} = K \cdot B_{sc}$. In our analysis, we assume a single user per beam, which represents the aggregation of the overall beam demand. The location of the user within the coverage area of each beam will be randomly selected for the performance evaluation and changed from realization to realization in Section IV. Furthermore, we assume that the beam size is fixed.

The channel vector from the satellite to the ith beam over the kth carrier is denoted by $\mathbf{h}_{i,k} = [h_{i,k}[1], h_{i,k}[2], \ldots, h_{i,k}[N]]^T$. Where $h_{i,k}[j]$ is a channel form the jth satellite feed towards the ith beam over the kth carrier. We denote $\mathbf{x}_k = [x_k[1], x_k[2], \ldots, x_k[N]]^T$ the assignment vector for carrier k, where $x_k[i] \in \{0, 1\}$ is a binary assignment

indicator, with $x_k[i] = 1$ indicating that carrier k is assigned to beam i. Similarly, the transmit power allocation vector for kth carrier is denoted as $\mathbf{p}_k = [p_k[1], p_k[2], \ldots, p_k[N]]^T$, where $p_k[i]$ is the transmit power of kth carrier towards the ith beam. The information symbols to be transmitted in the kth carrier are arranged in $\mathbf{s}_k = [s_k[1], s_k[2], \ldots, s_k[N]]^T$ with $\mathbb{E}[\mathbf{s}_k \mathbf{s}_k^H] = \mathbf{I}_N$. Hence, the received signal at ith beam from the kth carrier can be expressed as

$$y_k[i] = \mathbf{h}_{i,k}^T \sqrt{\mathbf{P}} \mathbf{X} \mathbf{s}_k + n_k[i], \tag{1}$$

where $\mathbf{P} = \text{diag}(\mathbf{p}_k)$ and $\mathbf{X} = \text{diag}(\mathbf{x}_k)$ are diagonal matrix of the power allocation vector and carrier assignment vector, respectively. The $n_k[i]$ denotes the additive white Gaussian noise at beam i for carrier k. By reformulating (1), we obtain

$$y_k[i] = \underbrace{\sqrt{p_k[i]} h_{i,k}[i] x_k[i] s_k[i]}_{\text{Desired Signal}}$$

$$+ \underbrace{\sum_{j=1, j \neq i}^{N} \sqrt{p_k[j]} h_{i,k}[j] x_k[j] s_k[j]}_{\text{Interference Signal}} + n_k[i]. \tag{2}$$

The channel coefficients $h_{i,k}[j]$ are defined as

$$h_{i,k}[j] = \frac{\sqrt{G_R G_i[j]}}{4\pi \frac{d_i}{\lambda}} e^{-\mathtt{i}\phi}, \tag{3}$$

where ϕ is the phase of the satellite antenna, G_R is the user terminal antenna gain, $G_i[j]$ denotes the gain from the jth satellite feed towards the ith beam and d_i is the slant range between the satellite and the user on the ith beam.

The signal-to-interference-plus-noise ratio (SINR) of the ith beam over kth carrier is given by

$$\gamma_{i,k}(\mathbf{p}_k, \mathbf{x}_k) = \frac{g_{i,k}[i] p_k[i] x_k[i]}{\sum_{j=1, j \neq i}^{N} g_{i,k}[j] p_k[j] x_k[j] + \sigma^2}, \tag{4}$$

where $g_{i,k}[j]$ denotes the channel power gain $g_{i,k}[j] = |h_{i,k}[j]|^2$ and $\sigma^2 = B_{sc} N_0$ is the noise power of $n_k[i]$. The N_0 is the noise power density. Hence, an upper-bound of the offered capacity at beam i in carrier k is given by the well-known Shannon capacity formula

$$C_{i,k} = B_{sc} \log_2(1 + \gamma_{i,k}(\mathbf{p}_k, \mathbf{x}_k)), \tag{5}$$

and an upper bound of the overall offered capacity at beam i considering the aggregation of all available carriers of the system is

$$C_i = \sum_{k=1}^{K} C_{i,k}. \tag{6}$$

III. PROPOSED CARRIER AND POWER ALLOCATION TO MAXIMIZE THE SATELLITE RESOURCE UTILIZATION

In this section, a resource allocation problem is formulated with the goal to satisfy the demand of each beam with minimum power and carrier utilization. For this, we select the sum of the total number of utilized carriers in the system and the total amount of consumed power as a joint objective

function for our optimization problem. The proposed optimization problem is formulated as follows,

$$\underset{\mathbf{x}_k, \mathbf{p}_k}{\text{minimize}} \sum_{i=1}^{N} \sum_{k=1}^{K} x_k[i] + \chi \sum_{i=1}^{N} \sum_{k=1}^{K} p_k[i]$$

$$\text{s.t. } R1 : \sum_{k=1}^{K} C_{i,k} \geq D_i, \forall_i,$$

$$R2 : \sum_{i=1}^{N} \sum_{k=1}^{K} p_k[i] \leq P_{total},$$

$$R3 : \sum_{k=1}^{K} p_k[i] \leq P_{max}, \quad \forall_i,$$

$$R4 : x_k[i] \in \{0, 1\}, \forall_i, \quad \forall_k,$$

$$R5 : p_k[i] \leq x_k[i] P_{max}, \quad \forall_i, \forall_k,$$

$$R6 : p_k[i] \geq 0, \forall_i, \quad \forall_k, \tag{7}$$

In (7), constraint $R1$ ensures that the total offered capacity in each beam satisfies the respective demand D_i. Constraint $R2$ provides the upper bound for the transmit power given by the total available power at the satellite P_{total}. In addition, we restrict the maximum power to be transmitted per beam by P_{max}. Furthermore, the carrier assignment $x_k[i]$ is a binary variable as indicated by $R4$. Constraint $R6$ ensures that the allocated power is non-negative. Constraint $R5$ guarantees that the power is allocated to beam i in carrier k only if the carrier is assigned, i.e. $x_k[i] = 1$. The scaling factor $\chi \in (0, \infty)$ measured in Watt^{-1} describes the priority of power consumption with respect to the carrier utilization. Note that $R5$ allows us to reformulate $\gamma_{i,k}(\mathbf{p}_k, \mathbf{x}_k)$ as

$$\gamma_{i,k}(\mathbf{p}_k) = \frac{g_{i,k}[i] p_k[i]}{\sum_{j=1, j \neq i}^{N} g_{i,k}[j] p_k[j] + \sigma^2}. \tag{8}$$

Due to the non-linearity of the SINR and the binary carrier assignment, the constraints $R1$ and $R4$ are non-convex. The non-convexity of $R1$ and $R4$ causes the optimization problem in (7) to be non-convex. In particular, the problem (7) corresponds to a non-convex mixed-integer program. Hence, no globally optimal solution for this problem can be obtained using the well-known tools of convex optimization, cf. [37].

Instead, we propose a sub-optimal method by splitting the non-convex optimization problem into two more tractable sub-problems. Despite being non-convex, these problems can be efficiently solved using the existing methods of successive convex approximation with close-to-optimum performance. The first sub-problem addresses the design of the carrier assignment variables $\mathbf{x}_k, \forall_k$, while the second sub-problem focuses on the overall consumed power minimization by designing the variables $\mathbf{p}_k, \forall_k$, based on the predefined carrier allocation obtained in the first step.

A. Carrier Assignment

In this section, we first obtain the number of carriers $K_i (1 \leq K_i \leq K)$ required for the ith beam to approximately match the requested demand. Next, we propose two algorithms to map the number of active carriers K_i into the respective variables $\mathbf{x}_k$, while minimizing the overall number of carriers.

Due to the assumed flat fading channel, we can exploit the fact that all the signal's spectral components will be affected by the channel in a similar manner.[1] The similarity of the channel at different carriers of the same ith beam allow us to express $\mathbf{h}_{i,k} \approx \hat{\mathbf{h}}_i$. Hence, it is likely that the SINR values in all carriers $k = 1, \ldots, K$ of beam i are similar, such that we can approximate (8) by $\hat{\gamma}_i(\mathbf{p})$ and (5) transforms into

$$C_i = \sum_{k=1}^{K} C_{i,k} = \sum_{k=1}^{K} B_{sc} \log_2(1 + \gamma_{i,k}(\mathbf{p}_k))$$

$$\approx K_i B_{sc} \log_2(1 + \hat{\gamma}_i(\mathbf{p})), \tag{9}$$

$$\text{with } \hat{\gamma}_i(\mathbf{p}) = \frac{g_i[i] p[i]}{\sum_{j=1, j \neq i}^{N} g_i[j] p[j] + \sigma^2}, \tag{10}$$

where $\mathbf{p} = [p[1], p[2], \ldots, p[N]]^T$ and $g_i[j] = |\hat{h}_i[j]|^2$. Here, $p[i]$ denotes the transmit power-per-carrier in the ith beam (same for all carriers within the beam). Hence, for a feasible interpretation of the results, the values of $p_k[i]$ must satisfy $p_k[i] \leq x_k[i] p[i]$.

Using (9), we formulate a similar problem as in (7) but replacing the sum of all carrier assignment variables $x_k[i]$ by the number of carriers K_i, $i = 1, \ldots, N$. The resulting problem is given by:

$$\underset{\{K_i, \forall_i\}, \mathbf{p}}{\text{minimize}} \sum_{i=1}^{N} K_i + \chi \sum_{i=1}^{N} K_i p[i]$$

$$\text{s.t. } V1 : K_i B_{sc} \log_2(1 + \hat{\gamma}_i(\mathbf{p})) \geq D_i, \quad \forall_i,$$

$$V2 : \sum_{i=1}^{N} K_i p[i] \leq P_{total},$$

$$V3 : K_i p[i] \leq P_{max}, \quad \forall_i,$$

$$V4 : K_i \in \mathcal{K}, \quad \forall_i,$$

$$V5 : p[i] \geq 0, \quad \forall_i, \tag{11}$$

Problem (11) is still non-convex because of the interference term in $\hat{\gamma}_i(\mathbf{p})$ of $V1$ and the integer value of K_i in $V4$. Hence, we propose a method to convexify (11). We start by approximating the integer constraint $V4$ as a continuous function in the range between 1 and K. Next, we replace $p[i]$ and K_i with the exponential functions $\exp(q[i])$ and $\exp(Z_i)$, respectively. Then, the constraints $V2$, $V3$, and $V4$ are replaced by $\{V2 : \sum_{i=1}^{N} \exp(q[i] + Z_i) \leq P_{total}\}$, $\{V3 : \exp(q[i] + Z_i) \leq P_{max}, \forall_i\}$, and $\{V4 : 0 \leq Z_i \leq \log(K), \forall_i\}$, respectively. Constraint $V1$ can be then reformulated as two constraints:

$$V1.1 : D_i \exp(-Z_i) - B_{sc} \log_2(1 + \exp(\alpha[i])) \leq 0, \quad \forall_i,$$

$$V1.2 : \exp(\alpha[i]) \leq \hat{\gamma}_i(\mathbf{p}), \quad \forall_i, \tag{12}$$

where $\exp(\alpha[i])$ is an exponential slack variable bounded below $\hat{\gamma}_i(\mathbf{p})$. By applying logarithm on $V1.2$ constraint

---

[1]Note that the atmospheric impairments usually affect the channel across a large signal spectrum in a similar way, such that the losses within the considered frequency band (e.g. $B_{tot} = 500$ MHz) can be viewed as sufficiently uniform.

and using (10)

$$V1.3: \alpha[i] - q[i] - \log(g_i[i])$$
$$+ \log\left(\sum_{j=1, j\neq i}^{N} g_i[j] \exp(q[j]) + \sigma^2\right) \leq 0, \quad \forall_i. \quad (13)$$

Since the log-sum-exp type of functions is convex (cf. [37]), (13) is convex, too. Unfortunately, constraint $V1.1$ remains non-convex. However, we observe that $V1.1$ contains a difference of convex functions. Thus, V1.1 can be treated as part of a DC Program. Correspondingly, the known method for solving this type of problems can be applied cf. [38]. The DC form of $V1.1$ is

$$V1.1: J_1(Z_i) - J_2(\alpha[i]) \leq 0, \quad \forall_i, \quad (14)$$

where both $J_1(Z_i) = D_i \exp(-Z_i)$ and $J_2(\alpha[i]) = B_{sc} \log_2(1 + \exp(\alpha[i]))$ are convex functions. The DC programming can be tackled using SCA algorithm [39] by approximating $J_2(\alpha[i])$. The first order approximation of $J_2(\alpha[i])$ in (14) is given by

$$\widetilde{J_2}(\alpha[i]) = J_2(\alpha[i]^{(l)}) + \nabla J_2(\alpha[i]^{(l)})(\alpha[i] - \alpha[i]^{(l)}), \quad (15)$$

where $\alpha[i]^{(l)}$ is the value of $\alpha[i]$ used in the lth iteration of SCA and

$$J_2(\alpha[i]^{(l)}) = B_{sc} \log_2(1 + \exp(\alpha[i]^{(l)})), \quad (16)$$

$$\nabla J_2(\alpha[i]^{(l)}) = B_{sc} \frac{1}{\log(2)} \left(\frac{\exp(\alpha[i]^{(l)})}{1 + \exp(\alpha[i]^{(l)})}\right). \quad (17)$$

The overall optimization problem (11) is reformulated as

$$\underset{Z_i, \mathbf{q}}{\text{minimize}} \sum_{i=1}^{N} \exp(Z_i) + \chi \sum_{i=1}^{N} \exp(q[i] + Z_i)$$
$$\text{s.t. } V1.1': J_1(Z_i) - \widetilde{J_2}(\alpha[i]) \leq 0, \quad \forall_i,$$
$$V1.3, \; V2, \; V3, \; V4, \quad (18)$$

Note that we removed $V5$ compared to (11) because $\exp(q[i])$ is always positive. In (18), $V1.1'$ is the first order approximation of $V1.1$. This problem is now convex and can be solved optimally. The iterative process to obtain the number of carriers required for each beam to match the traffic demand is detailed in **Algorithm 1**.

Since $\alpha[i]$ progressively increases in each iteration, we choose the value of the initial feasible point $\alpha[i]^{(0)}$ to be sufficiently small to satisfy the demand. For the results shown in this paper, we choose $\alpha[i]^{(0)} = 0.1$. The algorithm terminates when the SINR changes from one iteration to the other become negligible. In other words, when the absolute sum of the difference between $\exp(\alpha[i]^{(l)})$ and $\exp(\alpha[i]^{(l-1)})$ becomes very small (10^{-4} in this work).

Note that the solution $K_i = \exp(Z_i)$ of (18) in each iteration may have decimal values. Since K_i should be an integer number of carriers, we need a rounding procedure after completion of **Algorithm 1**. To ensure that beams receive enough carriers to satisfy their demand, we quantize K_i via $\widetilde{K_i} = \lceil K_i - \xi \rceil$, where $\lceil \cdot \rceil$ denotes the ceiling function and ξ is an auxiliary variable. The auxiliary variable ξ needs to be carefully chosen in order to maximize the system performance.

Next, we provide a complexity analysis of **Algorithm 1**. The procedure in **Algorithm 1** involves a complexity function

---

Algorithm 1 Optimization of the Number of Carriers

Input: feasible point $\alpha[i]^{(0)}, \forall i$;
$l \leftarrow 0$;
repeat
  $l \leftarrow l + 1$;
  Solve (18) to obtain $\alpha[i]^{(l)}$;
until $\left|\sum_i \left(\exp(\alpha[i]^{(l)}) - \exp(\alpha[i]^{(l-1)})\right)\right| \leq 10^{-4}$;
Output: Power per-carrier per-beam: $p[i] = \exp(q[i]), \forall_i$;
Output: Number of carriers per beam: $K_i = \exp(Z_i), \forall_i$;

$R(L)$ related to the number of iterations L and a complexity function $H(N)$ of the convex optimization procedure in (18) which depends on the number of beams N. The total complexity of **Algorithm 1** is the product of $R(L)$ and $H(N)$, such that the total computational complexity can be given by $\mathcal{O}(R(L)H(N))$. CVX tool solves the convex optimization (18) by constructing a polynomial approximation of its non-linear parts [40]. With first order polynomial approximation, the convex optimization (18) contains $2N$ decision variables and $5N + 1$ convex constraints. Then, the complexity of $H(N)$ is $\mathcal{O}((2N)^3(5N + 1))$. With $R(L) = L$, the total computational complexity of **Algorithm 1** is $\mathcal{O}(L(2N)^3(5N + 1))$ [41], [42].

In the following, we employ the optimized number of carriers $\widetilde{K_i}$ in order to obtain the carrier assignments $\mathbf{x}_k$. We propose two carrier assignment methods, both targeting the minimization of the number of operational carriers. Apart from the common goal of spectral efficiency, the two proposed methods follow different objectives which are detailed in the following.

1) Contiguous Carrier Assignment (CCA): In this mode, adjacent carriers are assigned to each beam. This is an important advantage of this mode, since the adjacent carriers can be aggregated if they need to be assigned to a high-demand user, thus substantially improves the power amplifier efficiency [43].

The detail carrier assignment procedure is explained in **Algorithm 2**. First, all values of $x_{i,k}$ are initially set to zero. Then, we fill the carrier assignments into vector $\mathbf{x}_k$ by setting $x_{i,k} = 1$, $k = 1, 2, \ldots, \widetilde{K_i}$. For example, assuming $K = 4$ and $N = 7$, and given the resulting set carrier assignment $\{\widetilde{K_1}, \ldots, \widetilde{K_7}\}$ equal to $\{1, 2, 1, 1, 3, 2, 1\}$, the output of **Algorithm 2** is shown in (19). Clearly, the proposed CCA compacts the carrier utilization regardless of the resulting interference.[2]

$$\begin{bmatrix} \mathbf{x}_1 & \mathbf{x}_2 & \mathbf{x}_3 & \mathbf{x}_4 \end{bmatrix} = \begin{bmatrix} 1 & 0 & 0 & 0 \\ 1 & 1 & 0 & 0 \\ 1 & 0 & 0 & 0 \\ 1 & 0 & 0 & 0 \\ 1 & 1 & 1 & 0 \\ 1 & 1 & 0 & 0 \\ 1 & 0 & 0 & 0 \end{bmatrix}. \quad (19)$$

---

[2]The latter is assumed to be controlled by the subsequent power optimization and by the fact the demand is satisfied in each beam even in case of full occupancy of each carrier according to the problem (11).

We can observe that **Algorithm 2** is very simple and its computational complexity is $\mathcal{O}(K_{max}N)$. Where K_{max} is the $\max\{\widetilde{K}_i\}$.

Algorithm 2 Contiguous Carrier Assignment Mode

Input: $\widetilde{K}_i$;
$x_{i,k} \leftarrow 0, \forall_i, \forall_k$;
$i \leftarrow 1$;
while $i \leq N$ **do**
    $x_{i,k} \leftarrow 1, 1 \leq k \leq \widetilde{K}_i$;
    $i \leftarrow i + 1$;
Output: $x_{i,k}, \forall_i, \forall_k$;

---

2) Interference Aware Carrier Assignment (IACA): In this mode, carriers are assigned such that a similar level of interference is received for all of the beams. This means that for each beam a contiguous carrier assignment may not be possible. To formulate the problem, we make use of the interference power received at the ith beam over the kth carrier, which is given by

$$I_k[i] = \sum_{j=1}^{N} w_{ji} x_k[j] \tag{20}$$

where $w_{ji} = p[j]g_i[j]$ is the interference "weight" from the jth beam towards beam i. Accordingly, our objective is to find the value of $x_k[j]$ that results in a fair interference distribution across beams. This problem is formulated as

$$\underset{\mathbf{x}_k}{\text{minimize}} \ \underset{k,i}{\max} \ \{I_k[i]\}$$

$$\text{s.t.} \ E1 : \sum_{k=1}^{K} x_k[i] = \widetilde{K}_i, \quad \forall_i,$$

$$E2 : x_k[i] \in \{0, 1\}, \forall_i, \quad \forall_k, \tag{21}$$

The optimization problem (21) follows a min-max formulation with the main goal to minimize the maximum of the interference metrics $I_k[i]$, $\forall_k$, $\forall_i$. Problem (21) considers two constraints, which are explained in the following. Constraint $E1$ ensures that each beam is assigned a total of $\widetilde{K}_i$ carriers. Constraint $E2$ indicates that $x_k[i]$ is a binary assignment variable.

The optimal solution for the problem (21) can be obtained via full search over all possible combinations of $x_k[i]$ for all k and i. However, full search imposes a very high computational complexity, especially when considering high dimensional systems with large numbers of carriers and beams. Hence, we propose a heuristic with polynomial computational time in the following.

Problem (21) is a fairness oriented design. Therefore, the interference distribution should be approximately uniformly distributed across beams. Denoting N_k as the number of beams that simultaneously operate in carrier k, we can intuitively set $N_k \approx (\sum_{i=1}^{N} \widetilde{K}_i)/K_{max}$, where $K_{max} = \max\{\widetilde{K}_i\}$. In order to avoid non-integer values of N_k, the

following approach for the calculation of N_k is proposed:

$$N_k = \begin{cases} \lfloor \dfrac{\sum_{i=1}^{N} \widetilde{K}_i}{K_{max}} \rfloor & k \leq \zeta \\[3mm] \lfloor \dfrac{\sum_{i=1}^{N} \widetilde{K}_i}{K_{max}} \rfloor + 1 & k > \zeta \end{cases} \tag{22}$$

with a threshold

$$\zeta = K_{max} - \left(\sum_{i=1}^{N} \widetilde{K}_i \mod K_{max} \right). \tag{23}$$

For a better understanding, we provide the following example to illustrate this approach. Given $\mathcal{K}_i = \{1, 2, 1, 1, 3, 2, 1\}$, we obtain $K_{max} = 3$ and a (23) equal to $\zeta = 3 - (11 \mod 3) = 1$. Therefore, for $k = 1$ we have $N_1 = \lfloor \frac{\sum_{i=1}^{N} \widetilde{K}_i}{K_{max}} \rfloor = \lfloor \frac{11}{3} \rfloor = 3$, and for $k = 2$ and $k = 3$ we have $N_2 = \lfloor \frac{\sum_{i=1}^{N} \widetilde{K}_i}{K_{max}} \rfloor + 1 = \lfloor \frac{11}{3} \rfloor + 1 = 4$ and $N_3 = \lfloor \frac{\sum_{i=1}^{N} \widetilde{K}_i}{K_{max}} \rfloor + 1 = \lfloor \frac{11}{3} \rfloor + 1 = 4$, respectively.

Algorithm 3 Interference Aware Carrier Assignment (IACA)

Input: $\widetilde{K}_i, \forall_i$; $\mathcal{N} = \{1, \ldots, N\}$; $x_{i,k} \leftarrow 0, \forall_i, \forall_k$;
$K_{max} \leftarrow \max(\widetilde{K}_i)$; $k \leftarrow 1$; $\mathcal{V}_k \leftarrow \emptyset, \forall_k$;
Find N_k using (22);
while $K_{max} \geq 1$ **do**
    $\mathcal{U}_k^1 \leftarrow \emptyset$;
    $\mathcal{U}_k^2 \leftarrow \emptyset$;
    $\mathcal{U}_k^1 \leftarrow \{i : \widetilde{K}_i = K_{max}\}$;
    $\mathcal{V}_k \leftarrow \mathcal{U}_k^1$;
    if $|\mathcal{V}_k| \neq N_k$ **then**
        $m \leftarrow \underset{i \in \mathcal{N}}{\max} \ \{w[i]\}$;
        $\mathcal{V}_k \leftarrow \{\mathcal{V}_k \cup m\}$;
        $\Phi \leftarrow N_k - |\mathcal{V}_k|$;
        while $\Phi > 0$ **do**
            $v \leftarrow \underset{i \in \mathcal{N}, i \notin \mathcal{V}_k}{\min} \ \{w_{im}\}$;
            $\mathcal{U}_k^2 \leftarrow \{\mathcal{U}_k^2 \cup v\}$;
            $\Phi \leftarrow \Phi - 1$;
        $\mathcal{V}_k \leftarrow \{\mathcal{V}_k \cup \mathcal{U}_k^2\}$;
    $x_{i,k} \leftarrow 1, \forall_i, i \in \mathcal{V}_k$;
    $K_{max} \leftarrow K_{max} - 1$;
    $\widetilde{K}_i \leftarrow \widetilde{K}_i - 1, i \in \mathcal{V}_k$;
    $k \leftarrow k + 1$;
    $\mathcal{N} \leftarrow \mathcal{N} \setminus \{m : \mathcal{K}_i \leq 0, \forall_i\}$;
Output: $x_{i,k}, \forall_i, \forall_k$;

The proposed heuristic for the IACA method, presented in **Algorithm 3**, makes use of N_k and the overall interference seen by beam i, which is defined as,

$$w[i] = \sum_{j=1}^{N} w_{ji}. \tag{24}$$

The main steps of **Algorithm 3** are summarized below.
1) Focusing on carrier k, we define $\mathcal{U}_k^1$ as the set including the beams whose $\widetilde{K}_i = K_{max}$. The beams in $\mathcal{U}_k^1$ are

selected to operate on carrier k. We record the beams assigned to carrier k with the set $\mathcal{V}_k = \mathcal{U}_k^1$. If the cardinality of $\mathcal{V}_k$ is equal to N_k, the assignment of carrier k is completed and the algorithm jumps to step (5). Otherwise, the algorithm continues with step (2).

2) Focusing on carrier k, the beam with higher overall interference, i.e. $m = \max\limits_{i \in \mathcal{N}} \{w[i]\}$, $\mathcal{N} = \{1, \ldots, N\}$, is selected to operate on such carrier, i.e. $\mathcal{V}_k = \mathcal{V}_k \cup \{m\}$.

3) Finally, the $\Phi = N_k - |\mathcal{V}_k|$ beams (if any) providing minimum overall interference to beam m are set to operate in carrier k, i.e. $\min\limits_{j, j \notin \mathcal{V}_k} \{w_{jm}\}$. Denoting these beams with the set $\mathcal{U}_k^2$, the set of beams assigned to carrier k expands as $\mathcal{V}_k = \mathcal{V}_k \cup \mathcal{U}_k^2$.

4) The carrier assignment vector $\mathbf{x}_k$ is updated as follows: $x_k[i] = 1$ for $i \in \mathcal{V}_k$.

5) For carrier $k + 1$ the same procedure (1-4) is followed after performing the following updates:

   a) The variables $\widetilde{K}_i$ are updated as $\widetilde{K}_i \leftarrow \widetilde{K}_i - 1$ for $i \in \mathcal{V}_k$. By definition, the variable K_{max} needs to be updated as well with $K_{max} - 1$.

   b) Remove the beams whose $\widetilde{K}_i = 0$ from the set $\mathcal{N}$, $\mathcal{N} = \mathcal{N} \setminus \{m\}$.

The complexity of **Algorithm 3** has a while loop with K_{max} and Φ times iteration. It required also N iteration to perform step 1 and step 2. Furthermore, it needs N_k iteration for step 4 and step 5 of a and b. Then, the complexity of **Algorithm 3** is $\mathcal{O}\left(2NK_{max} + \Phi K_{max} + 3N_k K_{max}\right)$.

B. Power Optimization for Active Carriers

After having optimized the carrier assignment $\mathbf{x}_k$ and obtained an upper-bound on the power per carrier in each beam $p[i]$, in this section we focus on the refinement of the power allocation via optimization of the transmit power per beam and per carrier $p_k[i]$. The optimization problem is formulated as follows,

$$\begin{aligned}
&\underset{\mathbf{p}_k}{\text{minimize}} \sum_{i=1}^{N} \sum_{k=1}^{K} p_k[i] \\
&\text{s.t. } R1, R2, R3, R6, \\
&\quad R7 : p_k[i] \leq x_k[i] p[i], \forall_i, \quad \forall_k,
\end{aligned} \tag{25}$$

The optimization problem (25) is non-convex because of constraint $R1$. However, similar to (11), this constraint can be reformulated in terms of DC programming and solved using SCA. By adding a lower bound exponential slack variable $\exp(\beta_k[i])$, replacing the power $p_k[i]$ by $\exp(q_k[i])$, and applying of SCA, the problem in (25) can be formulated as:

$$\begin{aligned}
&\underset{\{q_k[i], \forall_i\}}{\text{minimize}} \sum_{i=1}^{N} \sum_{k=1}^{K} \exp(q_k[i]) \\
&\text{s.t. } R1.3 : \beta_k[i] - q_k[i] - \log(g_{i,k}[i]) \\
&\quad + \log\left(\sum_{j=1, j \neq i}^{N} g_{i,k}[j] \exp(q_k[j]) + \sigma^2\right) \leq 0, \forall_i, \quad \forall_k, \\
&\quad R1.4 : D_i - \widetilde{Q}(\boldsymbol{\beta}) \leq 0,
\end{aligned}$$

$$R2 : \sum_{i=1}^{N} \sum_{k=1}^{K} \exp(q_k[i]) \leq P_{total},$$

$$R3 : \sum_{k=1}^{K} \exp(q_k[i]) \leq P_{max}, \quad \forall_i,$$

$$R7 : \exp(q_k[i]) \leq x_k[i] p[i], \quad \forall_i, \; \forall_k, \tag{26}$$

where $\widetilde{Q}(\boldsymbol{\beta})$ is the first-order approximation of $Q(\boldsymbol{\beta})$ and we removed $R6$ because $\exp(q[i])$ is always positive. Note that the detail reformulation of the problem (25) is provided in appendix. Then, the problem (26) is convex and we obtain a solution using an iterative procedure based on SCA, which is shown in **Algorithm 4**. Similar to **Algorithm 1**, we initialize the variable $\exp(\beta_k[i]^{(0)}) = 0.1$ for all i corresponding to active carriers. Then, (26) is solved, which leads to a new value $\beta_k[i]^{(l+1)}$. The algorithm terminates when the absolute sum of the difference between $\exp(\beta_k[i]^{(l)})$ and $\exp(\beta_k[i]^{(l-1)})$ is below 10^{-4}, which indicates the convergence of the proposed algorithm.

Algorithm 4 Power Allocation

Input: feasible point $\beta_k[i]^{(0)}$;
$l \leftarrow 0$;
repeat
   $l \leftarrow l + 1$;
   Solve (26) to obtain $\beta_k[i]^{(l)}$;
until
$|\sum_i \sum_k \left(\exp(\beta_k[i]^{(l)}) - \exp(\beta_k[i]^{(l-1)})\right)| \leq 10^{-4}$;
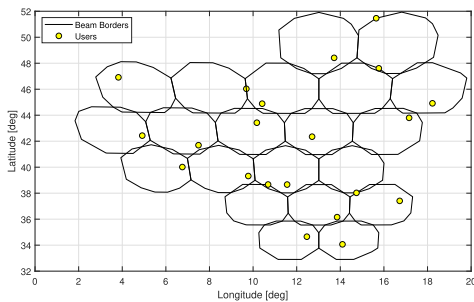Output: $p_k[i] = \exp(q_k[i]), \forall_i, \forall_k$

Similar to **Algorithm 1**, the complexity of the convex optimization of (26) with NK decision variables and $2N + 2NK + 1$ convex constraints is $(NK)^3(2N + 2NK + 1)$. Assuming the maximum number of iteration of the loop is L then the total complexity of **Algorithm 4** is $\mathcal{O}(L(NK)^3(2N + 2NK + 1))$ [41], [42]. Finally, the total complexity of carrier and power allocation of section III is the sum of the complexity of **Algorithm 1**, **Algorithm 4** and either of **Algorithm 2** or **Algorithm 3**. It is given by $\mathcal{O}\left(L(2N)^3(5N + 1) + L(NK)^3(2N + 2NK + 1) + NK_{max}\right)$ or $\mathcal{O}\left(L(2N)^3(5N+1) + L(NK)^3(2N+2NK+1) + 2NK_{max} + \Phi K_{max} + 2N_k K_{max}\right)$ if **Algorithm 2** or **Algorithm 3** used, respectively. As a result, the complexity is a polynomial function. Hence, the proposed algorithm can be obtained from a computer in polynomial time.

IV. SIMULATION RESULTS

In this section, we evaluate the performance of the proposed Carrier and Power Allocation (CPA) via numerical simulations. Table II provides a summary of the key simulation parameters. The results shown in this section have been obtained from Monte Carlo realizations in which the locations of the user terminals were selected randomly from a uniform distribution within the considered beam coverage for each realization. An example of user locations for a single realization is depicted in Fig. 2. Note that, in principle, any number of beams

TABLE II

SYSTEM PARAMETERS

Parameter	Value
Satellite Orbit	13°E
Satellite Beam Pattern	Provided by ESA
Number of beams (N)	21
Number of carrier (K)	4, 7, 20
System Bandwidth (B_{tot})	500 MHz
Sub-carrier bandwidth (B_{SC})	125 MHz, 71.4 MHz, 25 MHz
Noise power density (N_0)	-204 dBW/Hz
Max. beam gain ($G_i[j]$)	51.8 dBi
User antenna gain (G_R)	39.8 dBi
Total available transmit power (P_{total})	1000W
Maximum power per beam (P_{max})	100W
Auxiliary variable(ξ)	0.1

Fig. 3. Comparison of complexity analysis of CCA and IACA.

Fig. 2. $N = 21$ beam scenario with an example of super-user distribution.

modes is computed in Fig. 3 for different values of N and K. For simplification, we choose $N \in \{7, 21\}$ and we vary the number of carriers K between 4 and 100. We approximate also $K_{max} \approx K$ and $N_k \approx N$. As expected, the computational complexity of IACA is shown to be much higher than that of CCA. In addition, we observed that high computational time is required for $N = 21$ compared with $N = 7$. For example, at $K = 20$ the complexity for $N = 7$ and $N = 21$ is 560 and 1680, respectively. Furthermore, the increment of N or/and K causes the complexity of both modes to increase. However, since the scenario of the system is stationary (resulting from the geostationary orbit and very slowly time-varying demands of the representative users), the algorithm does not need to be executed in real-time. Moreover, the forthcoming SatCom systems are expected to utilize cloud/edge computing technology, which can tolerate high computational complexities including the complexity of the proposed method.

Note: The results included in Section B and C are based on the CPA-IACA mode. This is because the difference between IACA and CCA mode is only in power consumption which does not affect any other performance metric.

can be selected for the performance evaluation. However, for this simulation, we considered 21 beams.

Table III shows the metrics that are used for the performance evaluation and for comparison purposes, we consider the following benchmark schemes:

1) *Uniform Power 4CR*: Four color reuse scheme with uniform power allocation i.e. $p_{s1}[i] = P_{total}/N$.

2) *Demand-based Power 4CR*: Four color reuse scheme with demand based non-uniform power allocation i.e. $p_{s2}[i] = \frac{\left(2^{\frac{D_i}{B_{sc}}} - 1\right)\sigma^2}{g_i[i]}$. Note that proper scaling is applied to $p_{s2}[i]$ to satisfy R2 and R3.

3) *[26]*: A joint carrier and power allocation which is proposed in [26]. The value of the fixed power allocation is $p_k[i] = P_{total}/K$.

A. Comparison of CPA-CCA and CPA-IACA

We compare the performance of the proposed CPA employing CCA and IACA methods. Table IV shows the AUP result of CCA and IACA for uniform demand ranging from 100 Mbps up to 850 Mbps. The results confirm that IACA outperforms CCA in terms of power consumption. In particular, it can be observed that the difference in consumed power $\Delta = (\text{AUP}_{\text{CCA}} - \text{AUP}_{\text{IACA}})$ is maximize with demand $D_i = 450$ Mbps, with a difference of $\Delta = 8.4$ W. The benefits are not significant with very low and very high demand because all beams tend to employ most of the active carriers.

The power reduction gain provided by IACA comes at the cost of computational complexity. The complexity comparison of CCA and IACA is shown in Fig. 3. The complexity of both
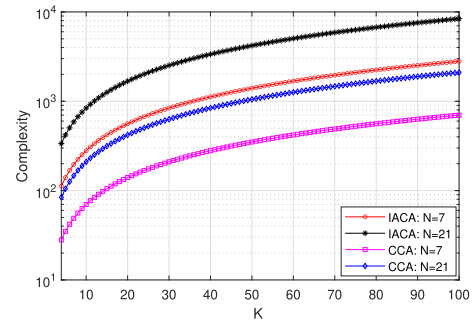
B. Comparison of CPA-IACA Versus Benchmarks Schemes

1) Homogeneous Demand: In this section, we assume that all beams have the same demand $D_i = D$, $\forall i$, and we vary the value of D between 100 and 1000 Mbps. Unless otherwise stated, $K = 20$ and $\chi = 1$ are assumed for all simulation results.

Fig. 4a compared the proposed CPA with benchmark schemes in terms of ASI. We observed that the proposed CPA improves user satisfaction by 36%, 100%, and 54.5%, compared with Uniform Power 4CR, Demand-based Power 4CR, and [26], respectively. The reason for the poor performance of the benchmark schemes is that the inter-beam interference is neglected to obtain power in Demand-based Power 4CR, whereas equal power per beam and fixed power per carrier are allocated in Uniform Power 4CR and [26]. In general, the performance of all schemes degrades with increasing demand. Moreover, this degradation results from the fact that for some channel realizations, it is physically impossible to satisfy the demand. The degradation of CPA, Uniform Power 4CR, and [26] starts at 600 Mbps, 450 Mbps and 300 Mbps, respectively. This indicates that the degradation of the proposed method starts much later compared with other

TABLE III
KEY PERFORMANCE INDICATORS

Average Satisfaction Index	$\text{ASI} = \frac{1}{M} \sum_{m=1}^{M} S[m]$, where M is the total number independent channel realization and $S[m]$ is satisfaction index at mth realization given by $S[m] = \begin{cases} 1 & C_i[m] \geq D_i[m], \forall_i \\ 0 & \text{otherwise} \end{cases}$
Average Used Power	For CPA and [26]: $\text{AUP} = \frac{1}{M} \sum_{m=1}^{M} \sum_{i=1}^{N} \sum_{k=1}^{K} p_k[i]$ For the Uniform Power 4CR and Demand-based Power 4CR: $\text{AUP} = \frac{1}{M} \sum_{m=1}^{M} \sum_{i=1}^{N} p_s[i]$ where $p_s[i]$ can be $p_{s1}[i]$ or $p_{s2}[i]$.
Average Used Carrier	$\text{AUC} = \frac{1}{M} \sum_{m=1}^{M} \sum_{i=1}^{N} \sum_{k=1}^{K} x_k[i]$
Average Used Bandwidth	$\text{AUB} = \frac{B_{tot}}{K}(\text{AUC})$
Average Unmet System Capacity	$\text{AUSC} = \frac{1}{M} \sum_{m=1}^{M} \sum_{i=1}^{N} max(D_i - C_i, 0)$
Average Unused Offered Capacity	$\text{AUOC} = \frac{1}{M} \sum_{m=1}^{M} \sum_{i=1}^{N} max(C_i - D_i, 0)$

TABLE IV
AVERAGE USED POWER BY CCA AND IACA MODES

Mbps	AUP (W)		Δ(W)	Mbps	AUP (W)		Δ(W)
	AUP_{CCA}	AUP_{IACA}			AUP_{CCA}	AUP_{IACA}	
100	14.6479	12.9347	1.7132	600	186.8440	181.8049	5.0391
150	22.9826	19.9344	3.0482	650	273.4531	270.3109	3.1422
200	31.2747	26.7994	4.4753	700	341.0006	338.6955	2.3052
250	39.1247	33.2019	5.9228	750	380.5707	378.4222	2.1485
300	44.5289	40.3182	4.2106	800	390.5772	388.4339	2.1433
350	53.0841	47.1946	5.8894	850	391.9236	389.7737	2.1499
400	62.4901	56.1644	6.3257				
450	76.5454	68.1941	8.3512				
500	94.3783	86.4235	7.9548				
550	122.2442	114.9515	7.2927				

schemes. Therefore, the proposed CPA method outperforms all benchmark schemes. Generally, we can apply the proposed technique to satisfy up to certain demands without precoding. Hence, for 21 beams, the proposed scheme can satisfy up to 600 Mbps per beam demand. Furthermore, thanks to the smart carrier and power assignment of the proposed scheme, a demand of 750 Mbps can be satisfied in more than 23% of cases.

The proposed technique not only shows a better demand matching compared to benchmark schemes, but also requires less overall transmit power. This can be achieved by allocating only as much power as needed to satisfy the demand. In contrast, no optimization of the power allocation is performed in Uniform Power 4CR and [26], such that the total transmit power is always large independently from the demand. In Demand-based Power 4CR, four color reuse leads to a low bandwidth utilization, which is compensated by an increased power consumption in order to provide sufficiently high capacity. Fig. 4b shows a comparison of the AUP for the proposed method and the benchmark schemes. All three benchmark schemes converge to the same AUP, which is equals the total available power P_{total}. In contrast, the proposed method converges to a different AUP, which is ≈ 4 dB less than for the benchmark schemes. Correspondingly, we observe a performance gain in terms of AUP, especially for high demand. For low demand, i.e. below 200 Mbps, the benchmark Demand-based Power 4CR seems to require less transmit power than the proposed method (by at most 1.5 dB). However, this is compensated by a better satisfaction index and utilization of number of carriers.

The proposed CPA scheme provides a lower AUSC metric compared to the benchmark schemes. Similarly to the observations of ASI, the drawback of the benchmark schemes lies in the suboptimality of the power allocation, which either neglects the inter-beam interference or is independent of the actual demand. The performance of the considered methods with respect to the AUSC is depicted in Fig. 4c. We observed that the AUSC is zero for the requested demand in the range 100 Mbps-600 Mbps, 100 Mbps-500 Mbps, and 100 Mbps-300 Mbps when CPA, Uniform Power 4CR, [26] is applied, respectively. The performance of Demand-based Power 4CR is above zero for all demands. As the demand increases the AUSC increases as well, with the proposed CPA providing the lowest AUSC results. Hence, for greater demands, precoding is recommended to compensate for the mismatch error. However, using the proposed algorithm, we can provide zero mismatch error for lower and medium demands.

Interestingly, the proposed CPA has no excess offered capacity since only as much power and as many carriers are allocated as needed in order to satisfy the demand. In contrast, in [26] the excess offered capacity is observed since the power and the carriers are fully used by the system whereas in Uniform Power 4CR the fixed power per carrier allocation leads to excess offered capacity at lower demands. Demand-based Power 4CR has no excess offered capacity since it provides a lower capacity than the requested demand, see Fig. 4a. The AUOC of the proposed CPA and the benchmark schemes are provided in Fig. 4d. The result of Uniform Power 4CR and [26] for demand below 800 Mbps and 500 Mbps, respectively indicates considerably high unused capacity. In contrast, for CPA and Demand-based Power 4CR the unused capacity is always equal to zero. In general, the performance of CPA in terms of demand matching is shown to be better compared to the benchmark schemes.

In addition to the mentioned advantages, the proposed scheme provides a more efficient utilization of carriers compared to the benchmark schemes. Both Uniform Power 4CR and Demand-based Power 4CR utilize four color reuse, which leads to the maximum utilization of the total frequency band. [26] requires much less carriers compared to the other two benchmark schemes with low demand due to the employed
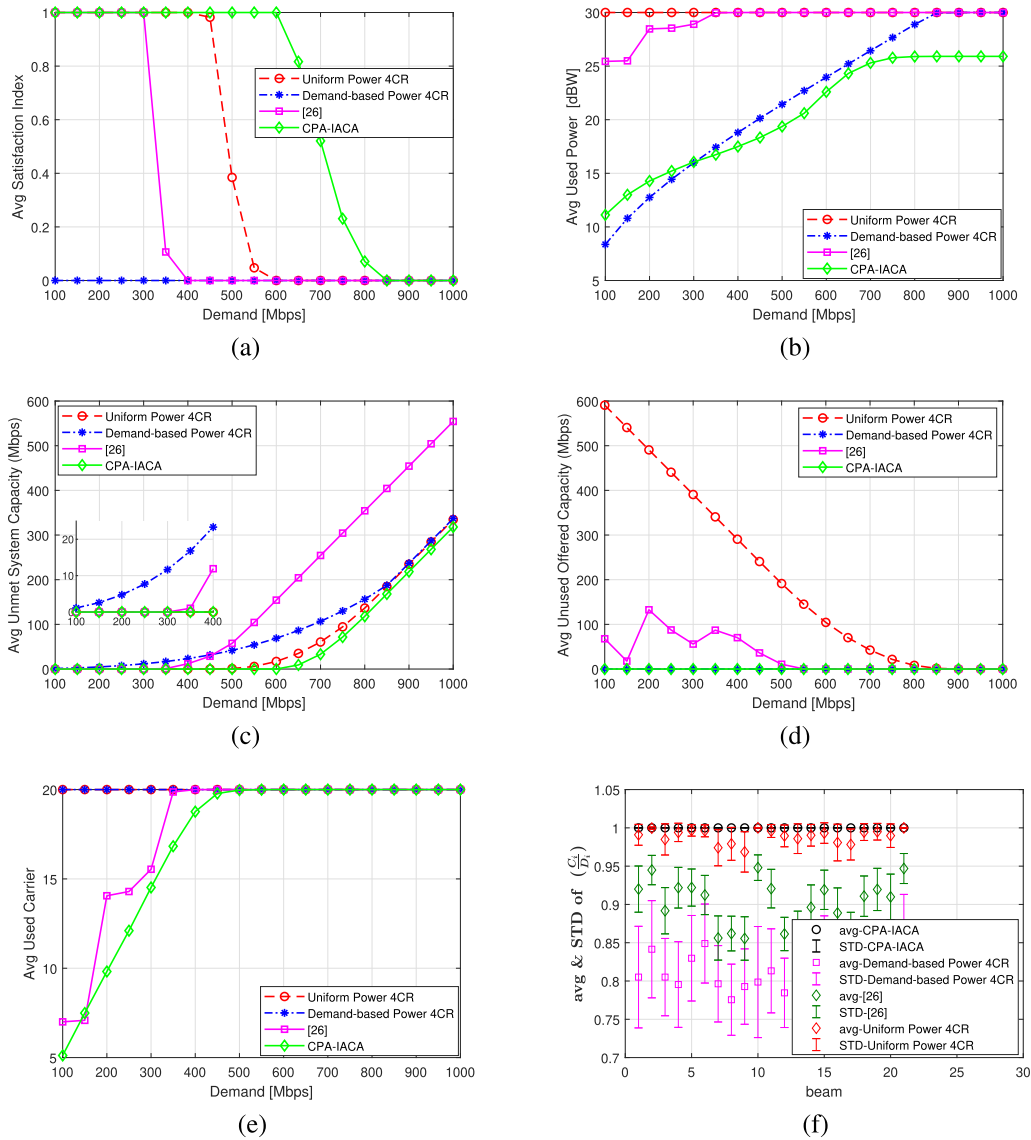
Fig. 4. Comparison of CPA and benchmark schemes for uniform demand per beam: (a) Average Satisfaction Index (ASI); (b) Average Used Power (AUP); (c) Average Unmet System Capacity (AUSC); (d) Average Unused Offered Capacity (AUOC); (e) Average Used Carrier (AUC); and (f) Average and standard division for $D_i = 550$Mbps.

carrier assignment. However, the power allocation is not optimal with [26], such that more carriers are assigned than actually needed to satisfy the demand. In contrast, the proposed CPA optimizes jointly the allocated power and the carrier assignment in aggressive frequency reuse mode. Hence, the required number of carriers is not overestimated with CPA. This leads to a better bandwidth utilization. Fig. 4e depicts the AUC of CPA and the benchmark schemes. As the demand increases, the number of used carriers increases for CPA and [26] while Uniform Power 4CR and Demand-based Power 4CR always operate with the maximum number of carriers. The results shown in Fig. 4e confirm that the proposed CPA-IACA scheme is able to satisfy the demands with much lower number of carriers than the benchmark schemes. For illustration, at 100Mbps, the average number of carrier used by CPA, Uniform Power 4CR, Demand-based Power 4CR and [26] are 5, 20, 20 and 7 respectively. As the

demand increases, all schemes converge to the total number of carriers K.

We have evaluated the standard deviation (STD) of the demand satisfaction expressed as C_i/D_i. The proposed algorithm is designed to match the offered capacity with demand per beam while using minimum power and a few carriers. Correspondingly, the demand satisfaction is mostly uniform across the beams, which results in a low standard deviation of the per beam demand. The results are depicted in Fig. 4f which shows how the standard deviation varies for each channel realization from its average (avg). We observe that the proposed method has a lower standard deviation compared to all benchmark schemes for the per beam demand ranging up to 550 Mbps. For example, at beam 10 of $D_i = 550$Mbps, the STD of the CPA, Uniform Power 4CR, Demand-based Power 4CR and [26] is 0, 0.0404, 0.0971, and 0.0581, respectively.
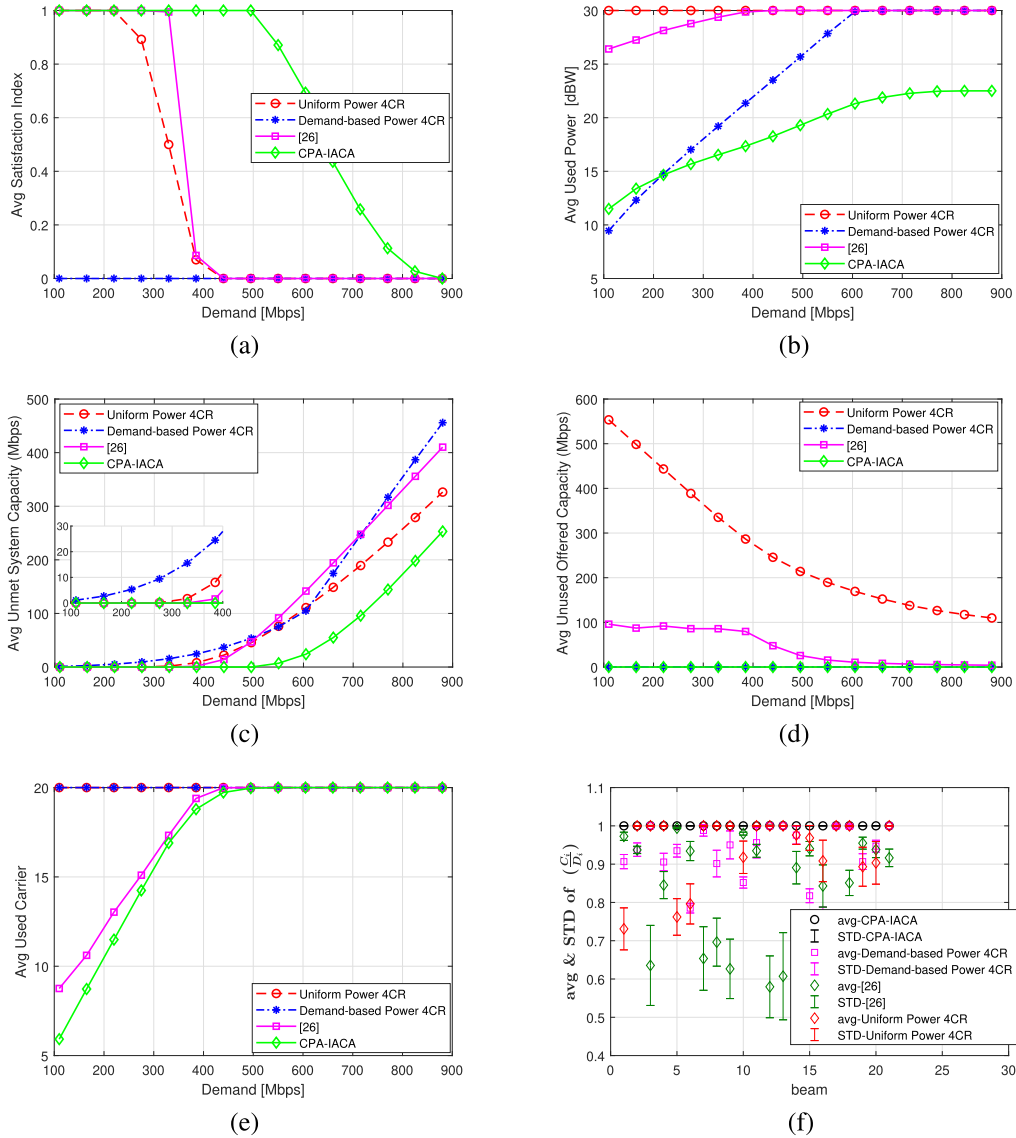
Fig. 5. Comparison of CPA and benchmark schemes for heterogeneous per beam: (a) Average Satisfaction Index (ASI); (b) Average Used Power (AUP); (c) Average Unmet System Capacity (AUSC); (d) Average Unused Offered Capacity (AUOC); (e) Average Used Carrier (AUC); and (f) Average and standard division for $D_i = iY[8]$ Mbps.
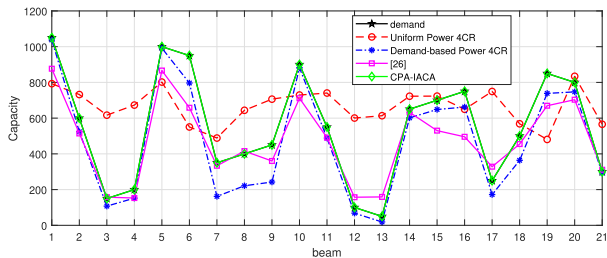

Fig. 6. The offered capacity per beam of all schemes with respect to individual demand for a single user location realization.

2) Heterogeneous Demand: In this section we compare the proposed scheme with the benchmark schemes in presence of spatially heterogeneous traffic demand. We choose $D_i = iY[v], \forall_i$ and $Y = [10, 15, 20, 25, 30, 35, 40, 45, 50, 55, 60, 65, 70, 80]$ in Mbps. Here, index i provides the scaling of the basic demand, which corresponds to the v-th element of Y. These

demands are carefully chosen to accommodate hot-spot beams (high demand), warm-spot beams (moderate demand), and cold-spots (low demand), cf. [44]. For the clarity of exposition we plot the performance metrics with respect to the average demand among all beams,[3] i.e. $\widetilde{D}[v] = \frac{\sum_i^N D_i}{N}, \forall_v$.

The results for the ASI, AUSC and AUOC are shown in Fig. 5a, Fig. 5c and Fig. 5d, respectively. Again, the results confirm the superiority of the proposed scheme over the benchmark schemes in terms of demand satisfaction and

---

[3]Note that we do not average the demand per beam for the resource allocation. However, we use the average demand to represent the distribution of demands. For instance, for $v = 1$ the average demand per beam is $\widetilde{D}[1] = \frac{\sum_i^N D_i}{N} = 110$ Mbps which represents the demand of all beams, i.e. the 21 beams would have the respective demands [10, 20, 30, 40, 50, 60, 70, 80, 90, 100, 110, 120, 130, 140, 150, 160, 170, 180, 190, 200, 210] Mbps. Hence, by saying that the average is 110 Mbps, we actually mean the distribution above.
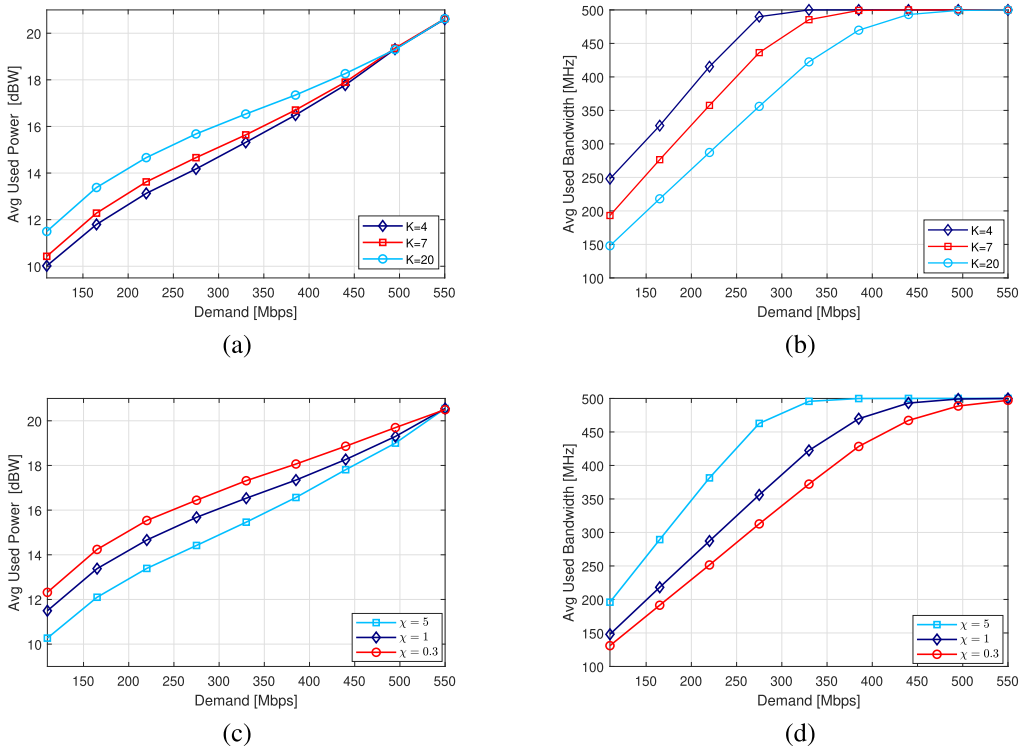
(a)

(b)

(c)

(d)

Fig. 7.   CPA for different K and χ values: (a) and (c) Average Used Power (AUP); (b) and (d) Average Used Bandwidth (AUB).

unmet/unused capacity. Furthermore, Fig. 5f shows the proposed CPA has lower standard deviation compared to the benchmark schemes. To emphasize that there is no averaging of the demand for the resource allocation, we show the simulation results per realization in Fig. 6. It can be observed that the benchmark schemes fail to match the per-beam demand, while the proposed method properly optimizes the system resource to satisfy the demand.

Regarding the satellite resource utilization, the AUP and AUC of CPA and benchmark schemes for non-uniform demand are shown in Fig. 5b and Fig. 5e. Similar to uniform demand the overall transmit power used by CPA is less compared to the benchmark schemes. All the benchmark schemes converge to the total available power P_{total} whereas the proposed method converges to AUP ≈ 22.5 dB, which is 7.5 dB less than P_{total}. Below 220 Mbps, the transmit power of Demand-based Power 4CR is less compared to CPA. However, CPA provides better ASI with proper power assignment compared to Demand-based Power 4CR. The results of AUC in Fig. 5e confirms that the proposed scheme is able to employ much less carriers than the benchmark schemes for the demands below 500Mbps. For higher demands, the CPA and benchmark schemes reach the maximum number of carriers K.

C. CPA-IACA Parameter Sensitivity Analysis

In this section, we analysis different parameter sensitivity of the proposed scheme. We consider a heterogeneous demand $D_i = iY[v], \forall_i$. Note that similar results have been observed for homogeneous demand.

TABLE V

NUMBER OF CARRIERS VERSUS DEMAND (IN PERCENT)

Demand (Mbps)	Carriers (K_i)						
	1	2	3	4	5	6	7
110	0	30	69	1	0	0	0
165	0	0	23	67	10	0	0
220	0	0	0	21	59	20	0
275	0	0	0	0	20	48	32
330	0	0	0	0	1	19	80
385	0	0	0	0	0	1	99
440	0	0	0	0	0	0	100

1) Spectrum Usage: The average percentage of active carriers per-beam is shown in Table V with $K = 7$. We observe the evolution of the number of active carriers with increasing demand. When $\widetilde{D}[1] = 110$ Mbps, $K_i = 2$ carrier is used in 30% of cases while 69% require $K_i = 3$. Starting from $\widetilde{D}[4] = 275$ Mbps all 7 carriers are sometimes needed. Below demands of $\widetilde{D}[3] = 220$ Mbps, we observe that minimum 2 carriers are not needed to satisfy the demand. Generally, as the demand increases, the algorithm assigns more carriers to satisfy the requested demand until the full-frequency reuse is reached, where all carriers are used in all beams.

2) Bandwidth Granularity: In this section we show how the proposed solution behaves for different K values. We consider $K \in \{4, 7, 20\}$.

Fig. 7a and Fig. 7b, respectively, show the power consumption and bandwidth utilization of the proposed scheme for different values of K. We have observed that less bandwidth utilization and more power consumption for higher

values of K. This is because the K has more weight in the objective function of (11) compared to the power variable. Hence, the (11) forced to minimize K than the power variable, which results in more power consumption. In contrast, (11) gives more priority to minimize power for a lower value of K. Therefore, less power consumption and higher bandwidth utilization are observed. Generally, Figs. 7a and 7b indicate a trade-off between power consumption and bandwidth utilization. Hence, depending on the available resources, it is possible to select a suitable K, which may lead to a higher bandwidth or power consumption. However, this flexibility is only available for low traffic demands. Selecting a suitable value of K for a given satellite system depends on the satellite operator requirements and payload capabilities. However, we recommend that a lower value of K should be selected for lower demand services. This saves more power for the system. However, a higher value of K must be selected for higher demand satisfaction.

3) Scaling-Factor: In this section we show how the proposed solution behaves for different χ values. We consider $\chi \in \{5, 1, 0.3\}$.

Like bandwidth granularity, we observe a trade-off between power consumption and bandwidth utilization of the proposed scheme for different values of χ. The average power used and the average used bandwidth are described in Fig. 7c and Fig. 7d, respectively. Higher power consumption with a few used bandwidth is observed for lower values of χ. This is because the proposed algorithm gives less priority to minimize power than the bandwidth. In contrast, with higher values of χ, the algorithm gives higher priority to minimize the power than the bandwidth. Hence, lower power consumption and more used bandwidth are observed for higher values of χ. In general, depending on system requirements and capabilities, satellite operators have to make a decision on the value of (χ) knowing that (i) high values of (χ) would prioritize power saving than spectrum utilization; and (ii) low values of (χ) would prioritize spectrum saving rather than power consumption. However, we recommended that if a high-demand service is required, a lower χ should be selected; otherwise, for lower demand request higher value of χ is good to select to save more power.

V. Conclusion

In this paper, we have proposed a novel carrier and power allocation method for flexible broadband GEO SatCom systems. The main objective of the method is to provide the best possible traffic matching while utilizing the least amount of resources. The formulated joint power and carrier assignment optimization problem turned out to be non-convex. Hence, we split the problem into two sub-problems i.e. carrier and power assignment, respectively. Since both sub-problems remain non-convex, we approximately solve them using successive convex approximation approach.

For the carrier assignment, two modes have been proposed, which aim at either minimizing the inter-beam interference in each carrier or assigning contiguous carriers for the future carrier aggregation. For the former method, an iterative method has been proposed. Both modes are compared in terms of

power consumption and complexity. We observe that the complexity of the interference minimization based mode is relatively high, which may become a burden, if low-complexity algorithms are required for the online operation. However, the forthcoming SatCom systems are expected to utilize cloud/edge computing technology, which can tolerate high computational complexities including the complexity of the proposed method.

A comparison of the proposed carrier and power allocation scheme with the most promising existing methods has been provided. We show that the proposed scheme outperforms the benchmark schemes in terms of average per-beam demand matching, average consumed power and bandwidth utilization.

While this work has focused on the conventional satellite antenna architecture with fixed beam-pattern, in our future work we plan to investigate the next generation of satellites equipped with active antenna systems, thus allowing reconfigurable beams on Earth. Furthermore, interference mitigation techniques can be considered on top of the proposed frequency allocation to further push the frequency reuse without a negative performance impact on the achievable capacity.

Appendix

By adding a lower bound exponential slack variable $\exp{(\beta_k[i])}$, we express $R1$ of problem (25) as,

$$R1.1 : D_i - \sum_{k=1}^{K} B_{sc} \log_2(1 + \exp{(\beta_k[i])}) \le 0, \quad \forall_i,$$
$$R1.2 : \exp{(\beta_k[i])} \le \gamma_{i,k}(\mathbf{p}_k), \forall_i, \quad \forall_k, \tag{27}$$

Both $R1.1$ and $R1.2$ in (27) are non-convex. In order to convexify $R1.2$ we replace the power $p_k[i]$ by $\exp{(q_k[i])}$. Applying the logarithm function on both sides of the equation and using (8), we can re-write it as follows:

$$R1.3 : \beta_k[i] - q_k[i] - \log{(g_{i,k}[i])}$$
$$+ \log \left(\sum_{j=1, j \ne i}^{N} g_{i,k}[j] \exp{(q_k[j])} + \sigma^2 \right) \le 0, \quad \forall_i, \forall_k, \tag{28}$$

In the following, we denote $\boldsymbol{\beta} = \left[\beta_1[i], \beta_2[i], \dots, \beta_K[i] \right]^T$. The constraint $R1.1$ contains a difference of convex functions. Thus, by approximating its concave part we obtain

$$R1.4 : D_i - \widetilde{Q}(\boldsymbol{\beta}) \le 0, \quad \forall_i, \tag{29}$$

where $\widetilde{Q}(\boldsymbol{\beta})$ is the first-order approximation of $Q(\boldsymbol{\beta})$:

$$\widetilde{Q}(\boldsymbol{\beta}) = Q(\boldsymbol{\beta}^{(l)}) + \nabla Q(\boldsymbol{\beta}^{(l)})(\boldsymbol{\beta} - \boldsymbol{\beta}^{(l)}), \tag{30}$$
$$Q(\boldsymbol{\beta}^{(l)}) = \sum_{m=1}^{K} B_{sc} \log_2(1 + \exp(\beta_m[i]^{(l)})), \tag{31}$$

$$\nabla Q(\boldsymbol{\beta}^{(l)}) = \frac{1}{\log(2)} \begin{bmatrix} \dfrac{\exp(\beta_1[i]^{(l)})}{1 + \exp(\beta_1[i]^{(l)})} \\ \vdots \\ \dfrac{\exp(\beta_K[i]^{(l)})}{1 + \exp(\beta_K[i]^{(l)})} \end{bmatrix}^T . \qquad (32)$$

Since the approximation of $Q(\boldsymbol{\beta})$ is repeated iteratively by the SCA algorithm, we denote $\boldsymbol{\beta}^{(l)}$ the value of $\boldsymbol{\beta}$ in lth iteration.

REFERENCES

[1] T. S. Abdu, E. Lagunas, S. Kisseleff, and S. Chatzinotas, "Carrier and power assignment for flexible broadband GEO satellite communications system," in *Proc. IEEE 31st Annu. Int. Symp. Pers., Indoor Mobile Radio Commun.*, Aug. 2020, pp. 1–7.

[2] S. K. Sharma, S. Chatzinotas, and P.-D. Arapoglou, *Satellite Communications in the 5G Era*. Edison, NJ, USA: IET Digital Library, 2018.

[3] O. Kodheli *et al.*, "Satellite communications in the new space era: A survey and future challenges," *IEEE Commun. Surveys Tuts.*, vol. 23, no. 1, pp. 70–109, 1st Quart., 2021.

[4] H. Fenech, A. Tomatis, S. Amos, V. Soumpholphakdy, and J. L. Serrano Merino, "Eutelsat HTS systems," *Int. J. Satell. Commun. Netw.*, vol. 34, no. 4, pp. 503–521, Jul. 2016. [Online]. Available: https://onlinelibrary.wiley.com/doi/abs/10.1002/sat.1171

[5] H. Fenech, A. Sonya, A. Tomatis, V. Soumpholphakdy, and J. L. S. Merino, "Eutelsat quantum: A game changer," in *Proc. 33rd AIAA Int. Commun. Satell. Syst. Conf. Exhib.*, 2015, pp. 1–10. [Online]. Available: https://arc.aiaa.org/doi/abs/10.2514/6.2015-4318

[6] *ESA FlexPreDem Project: Demostrator of Precoding Techniques for Flexible Broadband Systems*. Accessed: Dec. 2019. [Online]. Available: https://artes.esa.int/projects/flexpredem

[7] *ESA CADSAT Project: Carrier Aggregation in Satellite Communication Networks*. Accessed: Dec. 2019. [Online]. Available: https://artes.esa.int/projects/cadsat

[8] C. Braun, A. M. Voicu, L. Simic, and P. Mahonen, "Should we worry about interference in emerging dense NGSO satellite constellations?" in *Proc. IEEE Int. Symp. Dyn. Spectr. Access Netw. (DySPAN)*, Nov. 2019, pp. 1–10.

[9] C. N. Efrem and A. D. Panagopoulos, "Dynamic energy-efficient power allocation in multibeam satellite systems," *IEEE Wireless Commun. Lett.*, vol. 9, no. 2, pp. 228–231, Feb. 2020.

[10] H. Fenech, S. Amos, A. Hirsch, and V. Soumpholphakdy, "VHTS systems: Requirements and evolution," in *Proc. 11th Eur. Conf. Antennas Propag. (EUCAP)*, Mar. 2017, pp. 2409–2412.

[11] (Mar. 2017). *EUTELSAT 172B Satellite: On the Road to Kourou*. Accessed: Dec. 2019. [Online]. Available: https://news.eutelsat.com/pressreleases/eutelsat-172b-satellite-on-the-road-to-kourou-1857558

[12] (Apr. 2017). *SES and Thales Unveil Next Generation Capabilities On-Board SES-17*. Accessed: Feb. 2020. [Online]. Available: https://www.ses.com/press-release/ses-and-thales-unveil-next-generation-capabilities-onboard-ses-17

[13] S. Kisseleff, E. Lagunas, T. S. Abdu, S. Chatzinotas, and B. Ottersten, "Radio resource management techniques for multibeam satellite systems," *IEEE Commun. Lett.*, early access, Oct. 23, 2020, doi: 10.1109/LCOMM.2020.3033357.

[14] *SES-17 Satellite*. Accessed: Dec. 2020. [Online]. Available: https://www.ses.com/press-release/ses-and-thales-unveil-next-generation-capabilities-onboard-ses-17

[15] *Eutelsat Quantum Satellite*. Accessed: Dec. 2020. [Online]. Available: https://spacenews.com/intelsat-to-market-half-of-capacity-on-eutelsats-quantum-satellite/

[16] *Kythera Partners With SES*. Accessed: Dec. 2020. [Online]. Available: https://www.ses.com/press-release/ses-enhance-and-expand-o3b-mpower-system -capabilities-dynamic-software-innovation

[17] K. Roth, H. Pirzadeh, A. L. Swindlehurst, and J. A. Nossek, "A comparison of hybrid beamforming and digital beamforming with low-resolution ADCs for multiple users and imperfect CSI," *IEEE J. Sel. Topics Signal Process.*, vol. 12, no. 3, pp. 484–498, Jun. 2018.

[18] A. I. Aravanis, B. Shankar M. R., P.-D. Arapoglou, G. Danoy, P. G. Cottis, and B. Ottersten, "Power allocation in multibeam satellite systems: A two-stage multi-objective optimization," *IEEE Trans. Wireless Commun.*, vol. 14, no. 6, pp. 3171–3182, Jun. 2015.

[19] K. Kiatmanaroj, C. Artigues, L. Houssin, and F. Messine, "Frequency allocation in a SDMA satellite communication system with beam moving," in *Proc. IEEE Int. Conf. Commun. (ICC)*, Jun. 2012, pp. 3265–3269.

[20] U. Park, H. W. Kim, D. S. Oh, and B. J. Ku, "Flexible bandwidth allocation scheme based on traffic demands and channel conditions for multi-beam satellite systems," in *Proc. IEEE Veh. Technol. Conf. (VTC Fall)*, Sep. 2012, pp. 1–5.

[21] J. P. Choi and V. W. S. Chan, "Optimum power and beam allocation based on traffic demands and channel conditions over satellite downlinks," *IEEE Trans. Wireless Commun.*, vol. 4, no. 6, pp. 2983–2993, Nov. 2005.

[22] T. Qi and Y. Wang, "Energy-efficient power allocation over multibeam satellite downlinks with imperfect CSI," in *Proc. Int. Conf. Wireless Commun. Signal Process. (WCSP)*, Oct. 2015, pp. 1–5.

[23] N. K. Srivastava and A. K. Chaturvedi, "Flexible and dynamic power allocation in broadband multi-beam satellites," *IEEE Commun. Lett.*, vol. 17, no. 9, pp. 1722–1725, Sep. 2013.

[24] A. Destounis and A. D. Panagopoulos, "Dynamic power allocation for broadband multi-beam satellite communication networks," *IEEE Commun. Lett.*, vol. 15, no. 4, pp. 380–382, Apr. 2011.

[25] S. Kisseleff, B. Shankar, D. Spano, and J.-D. Gayrard, "A new optimization tool for mega-constellation design and its application to trunking systems," in *Proc. 37th Int. Commun. Satell. Syst. Conf.*, Nov. 2019, pp. 1–15.

[26] J. Lei and M. A. Vazquez-Castro, "Joint power and carrier allocation for the multibeam satellite downlink with individual SINR constraints," in *Proc. IEEE Int. Conf. Commun.*, May 2010, pp. 1–5.

[27] J. Lei and M. A. Vazquez-Castro, "Multibeam satellite frequency/time duality study and capacity optimization," *J. Commun. Netw.*, vol. 13, no. 5, pp. 472–480, Oct. 2011.

[28] A. Paris, I. Del Portillo, B. Cameron, and E. Crawley, "A genetic algorithm for joint power and bandwidth allocation in multibeam satellite systems," in *Proc. IEEE Aerosp. Conf.*, Mar. 2019, pp. 1–15.

[29] G. Cocco, T. de Cola, M. Angelone, Z. Katona, and S. Erl, "Radio resource management optimization of flexible satellite payloads for DVB-S2 systems," *IEEE Trans. Broadcast.*, vol. 64, no. 2, pp. 266–280, Jun. 2018.

[30] X. Alberti *et al.*, "System capacity optimization in time and frequency for multibeam multi-media satellite systems," in *Proc. 5th Adv. Satell. Multimedia Syst. Conf. 11th Signal Process. Space Commun. Workshop*, Sep. 2010, pp. 226–233.

[31] L. Lei, E. Lagunas, Y. Yuan, M. G. Kibria, S. Chatzinotas, and B. Ottersten, "Beam illumination pattern design in satellite networks: Learning and optimization for efficient beam hopping," *IEEE Access*, vol. 8, pp. 136655–136667, 2020.

[32] M. A. Vazquez *et al.*, "Precoding in multibeam satellite communications: Present and future challenges," *IEEE Wireless Commun.*, vol. 23, no. 6, pp. 88–95, Dec. 2016.

[33] E. Lagunas, S. Andrenacci, S. Chatzinotas, and B. Ottersten, "Cross-layer forward packet scheduling for emerging precoded broadband multibeam satellite system," in *Proc. 9th Adv. Satell. Multimedia Syst. Conf. 15th Signal Process. Space Commun. Workshop (ASMS/SPSC)*, Sep. 2018, pp. 1–8.

[34] V. Joroughi *et al.*, "Deploying joint beam hopping and precoding in multibeam satellite networks with time variant traffic," in *Proc. IEEE Global Conf. Signal Inf. Process. (GlobalSIP)*, Nov. 2018, pp. 1081–1085.

[35] G. Taricco and A. Ginesi, "Precoding for flexible high throughput satellites: hot-spot scenario," *IEEE Trans. Broadcast.*, vol. 65, no. 1, pp. 65–72, Mar. 2019.

[36] M. G. Kibria, E. Lagunas, N. Maturo, D. Spano, and S. Chatzinotas, "Precoded cluster hopping in multi-beam high throughput satellite systems," in *Proc. IEEE Global Commun. Conf. (GLOBECOM)*, Dec. 2019, pp. 1–6.

[37] S. Boyd and L. Vandenberghe, *Convex Optimization*. Cambridge, U.K.: Cambridge Univ. Press, 2004.

[38] X. Shen, S. Diamond, Y. Gu, and S. Boyd, "Disciplined convex-concave programming," 2016, *arXiv:1604.02639*. [Online]. Available: http://arxiv.org/abs/1604.02639

[39] T. Wang and L. Vandendorpe, "Successive convex approximation based methods for dynamic spectrum management," in *Proc. IEEE Int. Conf. Commun. (ICC)*, Jun. 2012, pp. 4061–4065.

[40] *The Successive Approximation Method*. Accessed: Feb. 2020. [Online]. Available: http://web.cvxr.com/cvx/doc/advanced.html#the-successive-approximation-method

[41] P. Gahinet, A. Nemirovski, A. J. Laub, and M. Chilali, *LMI Control Toolbox Users Guide*. Natick, MA, USA: MathWorks, 1995.

[42] A. Bandi, B. Shankar M. R, S. Chatzinotas, and B. Ottersten, "A joint solution for scheduling and precoding in multiuser MISO downlink channels," *IEEE Trans. Wireless Commun.*, vol. 19, no. 1, pp. 475–490, Jan. 2020.

[43] K. Pedersen, F. Frederiksen, C. Rosa, H. Nguyen, L. G. Garcia, and Y. Wang, "Carrier aggregation for LTE-advanced: Functionality and performance aspects," *IEEE Commun. Mag.*, vol. 49, no. 6, pp. 89–95, Jun. 2011.

[44] H. Al-Hraishawi, E. Lagunas, and S. Chatzinotas, "Traffic simulator for multibeam satellite communication systems," in *Proc. 10th Adv. Satell. Multimedia Syst. Conf. 16th Signal Process. Space Commun. Workshop (ASMS/SPSC)*, Oct. 2020, pp. 1–8.

Eva Lagunas (Senior Member, IEEE) received the M.Sc. and Ph.D. degrees in telecommunications engineering from the Polytechnic University of Catalonia (UPC), Barcelona, Spain, in 2010 and 2014, respectively. She was a Research Assistant with the Department of Signal Theory and Communications, UPC, from 2009 to 2013. In Summer 2009, she was a Guest Research Assistant with the Department of Information Engineering, Pisa, Italy. From November 2011 to May 2012, she held a visiting research appointment at the Center for Advanced Communications (CAC), Villanova University, Villanova, PA, USA. In 2014, she joined the Interdisciplinary Centre for Security, Reliability and Trust (SnT), University of Luxembourg, where she currently holds a research scientist position. Her research interests include radio resource management and general wireless networks optimization.

Tedros Salih Abdu (Graduate Student Member, IEEE) received the joint M.Sc. degree in electrical engineering from Pan African University and Jomo Kenyatta University of Agriculture and Technology, Kenya, in 2017. He is currently pursuing the Ph.D. degree with the Interdisciplinary Centre for Security, Reliability, and Trust (SnT), University of Luxembourg, where he is also a Doctoral Researcher. He has worked as a Lecturer with the Kombolcha Institute of Technology, Wollo University. His research interests include wireless communication technology, focusing on channel modeling, channel estimation, precoding, and resource optimization.

Steven Kisseleff (Member, IEEE) received the M.Sc. degree in information technology from the Technical University of Kaiserslautern, Germany, in 2011, and the Ph.D. degree in electrical engineering from the Friedrich-Alexander University of Erlangen-Nürnberg (FAU), Germany, in 2017.

He was a Research and Teaching Assistant with the Institute for Digital Communications, FAU, from October 2011 to July 2018. In 2012 and 2013, he was a Visiting Researcher at the State University of New York at Buffalo, USA, and at the Broadband Wireless Networking Lab, Georgia Institute of Technology, Atlanta, USA, respectively. In 2018, he joined the Interdisciplinary Centre for Security, Reliability and Trust (SnT), University of Luxembourg, where he currently holds a research scientist position. His research activities are mainly focused on the satellite communications, wireless power transfer, symbol-level precoding, and reconfigurable intelligent surfaces.

Symeon Chatzinotas (Senior Member, IEEE) received the M.Eng. degree in telecommunications from the Aristotle University of Thessaloniki, Thessaloniki, Greece, in 2003, and the M.Sc. and Ph.D. degrees in electronic engineering from the University of Surrey, Surrey, U.K., in 2006 and 2009, respectively. He is currently a Full Professor/ Chief Scientist I and the Co-Head of the SIGCOM Research Group at SnT, University of Luxembourg. In the past, he was a Visiting Professor at the University of Parma, Italy, and he was involved in numerous research and development projects for the National Center for Scientific Research Demokritos, the Center of Research and Technology Hellas, and the Center of Communication Systems Research, University of Surrey. He was a co-recipient of the 2014 IEEE Distinguished Contributions to Satellite Communications Award, the CROWNCOM 2015 Best Paper Award, and the 2018 EURASIC JWCN Best Paper Award. He has (co)authored more than 400 technical articles in refereed international journals, conferences, and scientific books. He is currently in the Editorial Board of the IEEE OPEN JOURNAL OF VEHICULAR TECHNOLOGY and the *International Journal of Satellite Communications and Networking*.